21. Hensel J C, Phillips T G, Thomas G A, in *Solid State Physics* Vol. 32 (Eds H Ehrenreich, F Seitz, D Turnbull) (New York: Academic Press, 1977) p. 88 [Translated into Russian (Moscow: Mir, 1980) p. 101]
22. Jeffries C D, Keldysh L V (Eds) *Electron-Hole Droplets in Semiconductors* (Modern Problems in Condensed Matter Sciences, Vol. 6) (Amsterdam: North-Holland, 1983) [Translated into Russian (Moscow: Nauka, 1988)]
23. Tikhodeev S G *Usp. Fiz. Nauk* **145** 3 (1985) [*Sov. Phys. Usp.* **28** 1 (1985)]
24. Keldysh L V, Sibeldin N N, in *Nonequilibrium Phonons in Nonmetallic Crystals* (Modern Problems in Condensed Matter Sciences, Vol. 16, Eds W Eisenmenger, A A Kaplyanskii) (Amsterdam: North-Holland, 1986) p. 455
25. Keldysh L V, Onishchenko T A *Pis'ma Zh. Eksp. Teor. Fiz.* **24** 70 (1976) [*JETP Lett.* **24** 59 (1976)]
26. Andryushin E A et al. *Pis'ma Zh. Eksp. Teor. Fiz.* **24** 210 (1976) [*JETP Lett.* **24** 185 (1976)]
27. Kavetskaya I V, Sibel'din N N, Tsvetkov V A *Zh. Eksp. Teor. Fiz.* **105** 1714 (1994) [*JETP* **78** 926 (1994)]
28. Kavetskaya I V, Sibeldin N N, Tsvetkov V A *Solid State Commun.* **97** 157 (1996)
29 Kavetskaya I V et al. *Zh. Eksp. Teor. Fiz.* **111** 737 (1997) [*JETP* **84** 406 (1997)]
30. Kanskaya L M, Kokhanovskiĭ S I, Seĭsyan R P *Fiz. Tekh. Poluprovodn.* **13** 2424 (1979)
31. Kavetskaya I V et al. *Zh. Eksp. Teor. Fiz.* **100** 2053 (1991) [*Sov. Phys. JETP* **73** 1139 (1991)]
32. Kavetskaya I V, Sibel'din N N, Tsvetkov V A *Fiz. Tverd. Tela* **34** 857 (1992) [*Sov. Phys. Solid State* **34** 458 (1992)]
33. Störmer H L, Martin R W *Phys. Rev. B* **20** 4213 (1979)
34. Kokhanovskiĭ S I, Thesis for Candidate of Physico-Mathematical Sciences (Leningrad: Ioffe Physico-Technical Institute, 1982)
35. Gel'mont B L et al. *Fiz. Tekh. Poluprovodn.* **11** 238 (1977)
36. Keldysh L V *Contemp. Phys.* **27** 395 (1986)
37. Silin A P, in *Electron-Hole Droplets in Semiconductors* (Modern Problems in Condensed Matter Sciences, Vol. 6, Eds C D Jeffries, L V Keldysh) (Amsterdam: North-Holland, 1983) p. 619; [Translated into Russian (Moscow: Nauka, 1988) p. 449]
38. Chernenko A V, Timofeev V B *Zh. Eksp. Teor. Fiz.* **112** 1091 (1997) [*JETP* **85** 593 (1997)]

PACS numbers: **41.20.–q**, **78.67.–n**

DOI: 10.1070/PU2003v046n09ABEH001657

Spontaneous atomic radiation in the presence of nanobodies

V V Klimov

1. Introduction

Due to the rapid development of nanotechnologies, it is important to know how nanobodies, i.e., bodies that are small compared to the emission wavelength, influence various optical phenomena. The corresponding subject is called *nanooptics* and plays a special role in optics, since optical effects in the vicinity of nanobodies are determined by the typical sizes of the nanobodies rather than the emission wavelength. At smaller spatial scales, the concentration of electromagnetic fields near the objects increases. Therefore, nanobodies can be efficiently used in nanotechnologies, in developing scanning microscopes with nanometer resolution, in nonlinear optical elements, and in other applications like control of fluorescence and spontaneous emission.

Enhancement or inhibition in the rate of spontaneous emission for an atom in a cavity, which was predicted in Refs [1, 2], was observed in a series of experimental works [3–10] where the cavity size was essentially larger than or comparable to the emission wavelength.

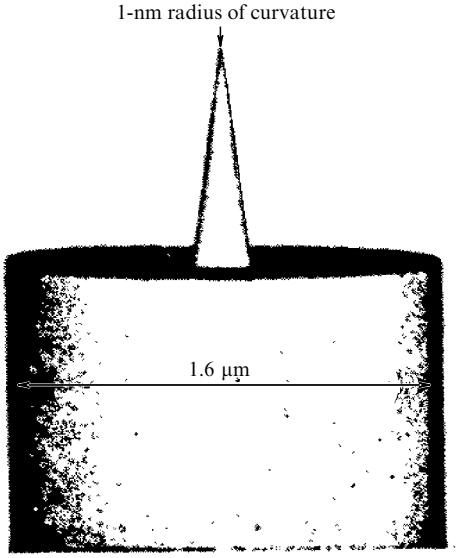

Figure 1. Photograph of a scanning microscope tip made by means of a tunnel electron microscope. The radius of tip curvature is about 1 nm [11, pp. 131–139].

In practice, however, it is often important to find out how nanobodies influence the spontaneous emission of an atom. Such problems arise first of all in the studies of isolated molecules by means of aperture and aperture-free scanning microscopes. Figure 1 shows a typical nanobody, namely the tip of an aperture-free scanning microscope [11]. Nanoparticles of various shapes are also used for controlling fluorescence [12]. In practice, it is sometimes important to elucidate the influence of nanofibres or nanowires on the spontaneous emission of atoms [13–16].

In the present work, we study the effect of nanobodies of various shapes (spherical, spheroidal, cylindrical, etc.) and a round nano-aperture on the spontaneous emission of an atom placed in their vicinity. Our aim is to find the conditions under which spontaneous emission of atomic particles can be efficiently controlled.

2. Theory of the spontaneous emission of atoms in the presence of nanobodies

If the interaction between the atom and the nanobody is weak, i.e., in the case of exponential radiative decay, the expression for the line width γ has the form [17, 18]

$$\frac{\gamma}{\gamma_0} = 1 + \frac{3}{2}\,\mathrm{Im}\,\frac{\mathbf{d}_0\,\mathbf{E}^R(\mathbf{r},\mathbf{r},\omega_0)}{d_0^2 k^3}\,, \qquad (1)$$

where $\mathbf{E}^R(\mathbf{r},\mathbf{r},\omega_0)$ describes the reflected field of the dipole $\mathbf{d}_0$ in the vicinity of the nanobody at the frequency ω_0 of the atom emission and at point $\mathbf{r}$ where the atom is placed. It can be found by solving the Maxwell equations. Other parameters in Eqn (1) are as follows: γ_0, the line width in vacuum, and $k = \omega_0/c$.

Expression (1) governs the total decay rate of an atom, i.e., the rate at which the radiated energy goes to infinity and is absorbed by the nanobody. It is valid for bodies made of any material. It is worth noting that relation (1) can be used for solving both classical and quantum-mechanical problems

[19 – 21]. Therefore, in order to find the spontaneous decay rate in the vicinity of a nanobody one is obliged to calculate the reflected field and analyze relation (1). Calculation of the reflected field is a complicated problem which sometimes has no analytical solution.

Dealing with nanobodies, it is often possible to take advantage of perturbation theory formulated in terms of the small parameter $ka = 2\pi a/\lambda$, where a is the typical size of the nanobody, and λ is the emission wavelength. This approach, also called the Rayleigh theory, gives the expression for the reflected field as a series expansion in powers of the wave vector k:

$$\frac{\mathbf{d}_0\mathbf{E}^{(R)}(\mathbf{r},\mathbf{r},\omega_0)}{d_0^2} = a_1(\mathbf{r}) + b_1(\mathbf{r})\,k + c_1(\mathbf{r})\,k^2 + \mathrm{i}d_1(\mathbf{r})\,k^3 + \ldots , \quad (2)$$

where the coefficients a_1, b_1, c_1, and d_1 can be found by solving the corresponding quasi-static problems. The first three terms describe near fields, while the higher-order terms correspond to radiation fields. Substituting expansion (2) into (1), we obtain the total rate of spontaneous decays nearby the nanobody in the form

$$\frac{\gamma}{\gamma_0} = \frac{3}{2}\,\mathrm{Im}\left(\frac{a_1(\mathbf{r})}{k^3} + \frac{b_1(\mathbf{r})}{k^2} + \frac{c_1(\mathbf{r})}{k}\right) + 1 + \frac{3}{2}\,\mathrm{Re}\,d_1(\mathbf{r}) + \ldots \quad (3)$$

In this expression, the first term differs from zero only in absorbing media and describes nonradiative losses. The second and the third terms can also be nonzero in the absence of absorption; they describe radiative losses. It follows that for finding nonradiative and radiative losses in the first approximation, it is sufficient to determine the coefficients a_1 and d_1, respectively. The term containing a_1 can be found by solving the quasi-static problem with a dipole source. Direct calculation of radiative losses described by the terms of a third-order in k seems to be a complicated problem. However, if the atom is placed close to the nanobody, radiation can be considered in a dipole approximation and the total dipole moment of the system 'atom + nanobody' can again be calculated by solving the quasi-static problem in the lowest approximation. Thus, in the case of nanobodies, radiative line width is given by the relation

$$\left(\frac{\gamma}{\gamma_0}\right)^{\text{radiative}} = \frac{|\mathbf{d}_{\text{tot}}|^2}{|\mathbf{d}_0|^2}\,, \quad (4)$$

where $\mathbf{d}_{\text{tot}}$ is the total dipole moment of the system 'atom + nanobody'.

Thus, variation of the spontaneous decay rate due to the presence of any nanobody that is small compared to the emission wavelength can be found by solving the quasi-static problem for a dipole in the vicinity of this nanobody.

Although the theoretical approaches considered above are based on the fundamental principles of quantum electrodynamics, it is preferable to test the results in experiment, since, sooner or later, the employment of the concept of nanobody permittivity will become inapplicable .

Experiments with isolated atoms in the vicinity of macroscopic bodies are extremely complicated and, at present, reliable experimental data have been obtained only for lifetimes of atoms and ions in the neighborhood of a partly reflecting flat surface [22, 23]. The results of these experiments have demonstrated perfect agreement with the theory down to nanometer distances.

3. Spontaneous emission of an atom in the vicinity of a nanosphere

If an atom is placed close to a nanosphere, spontaneous radiative decay rates can be found analytically for any size of the sphere and for any position of the atom [24 – 28].

In the case of a nanosphere, which is a sphere whose radius a is small with respect to the emission wavelength ($ka \to 0$), the radiation width of spectral line for an atom placed at the distance r from the center and having the radial orientation of the dipole moment can be calculated as follows

$$\left(\frac{\gamma}{\gamma_0}\right)^{\text{radiative}}_{\text{radial}} \underset{ka\to 0}{\longrightarrow} \left|1 + \frac{2(\varepsilon-1)}{\varepsilon+2}\left(\frac{a}{r}\right)^3\right|^2 + O\big((ka)^2\big)\,, \quad (5)$$

where ε is the permittivity of the sphere at the wavelength of the atomic radiation.

Relation (5) is valid for the most of practical cases. In the special case of plasmon resonance, when the condition $|\varepsilon + 2| \ll (ka)^2 \ll 1$ is satisfied, expression (5) is inapplicable. For nanospheres with $\varepsilon \approx -2$, instead of Eqn (5), we have

$$\left(\frac{\gamma}{\gamma_0}\right)^{\text{radiative}}_{\text{radial}} \overset{\varepsilon=-2,\,ka\to 0}{\longrightarrow} \frac{25}{4(ka)^4}\left(\frac{a}{r}\right)^6 . \quad (6)$$

Hence, one can see that in the case of plasmon resonance, essential enhancement of the spontaneous transition rate can be achieved due to the factor $(ka)^{-4}$.

If the atom is placed inside the nanosphere, the radiative decay rate is given by the expression

$$\left(\frac{\gamma}{\gamma_0}\right)^{\text{radiative}}_{\text{radial}} \underset{ka\to 0}{\longrightarrow} \frac{9}{|\varepsilon+2|^2} + O\big((ka)^2\big)\,, \quad (7)$$

which in the case of a plasmon resonance takes the form

$$\left(\frac{\gamma}{\gamma_0}\right)^{\text{radiative}}_{\text{radial}} \overset{\varepsilon=-2,\,ka\to 0}{\longrightarrow} \frac{25}{16(ka)^4}\,. \quad (8)$$

Note that the leading terms in formulas (7) and (8) do not depend on the position of the atom inside the sphere.

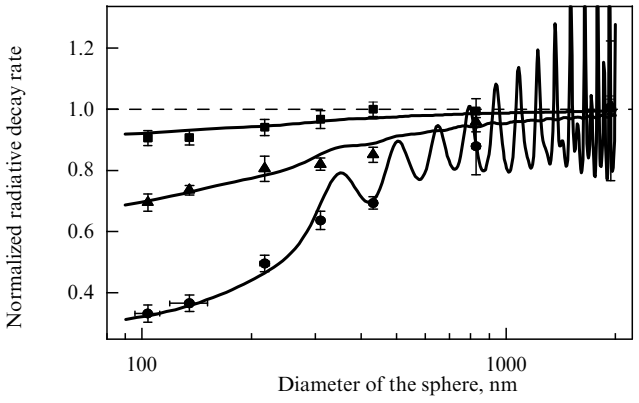

Figure 2. Radiative decay rates measured for an atom in polystyrene nanospheres placed into air (•), water (▲), and immersion oil (■) [29]. Solid lines show the results of theoretical investigations [24 – 28].

In general, the sphere has a strong influence on the radiative decay of an excited atom. If the nanosphere is insulating ($\varepsilon > 1$), the excitation energy is emitted in the form of photons, and the rate of this radiative decay can be increased or reduced several times depending on the orientation of the transition dipole moment. In the special case (plasmon resonance, $\varepsilon \approx -2$), the atomic decay remains radiative, i.e., the radiant energy goes to infinity in the form of photons, but the decay rate rises proportionally to the inverse fourth power of the sphere radius.

In Ref. [29], spontaneous radiation of Eu atoms placed in micro- and nanospheres was studied experimentally. Comparison of the experimental results with the theory (see Fig. 2) shows a good agreement in the range of nanospheres.

4. Spontaneous emission of an atom in the vicinity of a circular cylinder

This problem can be solved analytically for a cylinder of any size and for any position of the atom [30–32]. If the cylinder is of nanoscopic size, the situation becomes more complicated, because, in this situation, propagation of fundamental waveguide modes of any frequency is possible, and the energy of the atomic excitation can be radiated to infinity as spherical waves or be captured by the waveguide modes. In the particular case of an absorbing material, nonradiative decay is also possible.

Consider first an insulating cylinder (a nanofibre) with the permittivity $\varepsilon > 1$. For an atom with a radially aligned dipole moment, placed at a distance ρ from the axis of a cylinder with radius a, the radiative decay rate is given by

$$\left(\frac{\gamma}{\gamma_0}\right)_{\text{radial}}^{\text{radiative}} = \left|1 + \frac{\varepsilon - 1}{\varepsilon + 1}\,\frac{a^2}{\rho^2}\right|^2, \tag{9}$$

while for nonradiative decays, the rate is defined as

$$\left(\frac{\gamma}{\gamma_0}\right)_{\text{radial}}^{\text{nonradiative}} = -\frac{3}{\pi k^3}\sum_{m=0}^{\infty}(2-\delta_{m,0}) \times \int_0^{\infty} \mathrm{d}h h^2 K_m'^2(h\rho)\,\mathrm{Im}\,G_m(ha)\,, \tag{10}$$

where the coefficients $G_m(ha)$ have the form

$$G_m(s) = \frac{(\varepsilon - 1)\,I_m'(s)\,I_m(s)}{K_m'(s)\,I_m(s) - \varepsilon K_m(s)\,I_m'(s)}\,. \tag{11}$$

If the atom is placed very close to the surface, then a more simple expression can be obtained instead of Eqn (10). It is analogous to the expression for nonradiative decays in the vicinity of a flat surface:

$$\left(\frac{\gamma}{\gamma_0}\right)_{\text{radial}}^{\text{nonradiative}} = \mathrm{Im}\left(\frac{\varepsilon - 1}{\varepsilon + 1}\right)\frac{3}{16k^3(\rho - a)^3}\,. \tag{12}$$

In addition, the emitted photon can be captured by waveguide modes, so that

$$\left(\frac{\gamma}{\gamma_0}\right)_{\text{radial}}^{\text{guided}} = \frac{48\varepsilon^2}{(\varepsilon - 1)^2(ka)^6}\exp\left(-\frac{2}{(ka)^2}\,\frac{\varepsilon + 1}{\varepsilon - 1} + \ldots\right). \tag{13}$$

The energy captured by waveguide modes can form a significant part (up to 70%) of the total decay energy, but the radial localization of these modes becomes considerably worse with a decrease in the nanofibre radius.

In the case of a metal nanocylinder, i.e., a nanowire with $\mathrm{Re}\,\varepsilon < -1$, the rate of radiative decays is again described by expression (9), while the rate of decay into symmetric waveguide modes is given by the following expression

$$\left(\frac{\gamma}{\gamma_0}\right)_{\text{radial}}^{\text{guided}} = -3s^* I_0(s^*)\,K_1^2(s^*) \times \left\{(ka)^3 K_0(s^*)\,\frac{\mathrm{d}}{\mathrm{d}s}\left[I_0(s)\,K_1(s) + \varepsilon I_1(s)\,K_0(s)\right]_{s=s^*}\right\}^{-1}, \tag{14}$$

where s^* is the solution to the equation

$$s^2 = \frac{2}{(\varepsilon - 1)\left[\ln(s/2) + 0.577216\right]}\,.$$

Analyzing equation (14), one can show that due to the excitation of symmetric waveguide modes, a decrease in the nanowire radius can lead to a growth in the decay rate by several orders of magnitude.

We conclude that a nanocylinder, i.e., a cylinder whose radius is small compared to the emission wavelength, has an essential influence on the radiative decay of an excited atom. In the presence of a nanowire, the decay is mostly determined by the capture of radiation by symmetric waveguide modes, which leads to a considerable increase in the decay rate at small wire radii, provided that the transition dipole moment is aligned radially. In the case of an insulating cylinder, the decay process becomes more complicated: part of the energy is emitted to infinity in the form of photons, and the rest of the energy is transformed into that of nondecaying waveguide modes of the cylinder and, hence, is not emitted.

5. Spontaneous emission of an atom in the vicinity of a nano-aperture

In order to describe the operation of an aperture scanning microscope with a single molecule as the object under study, it is important to understand how spontaneous emission proceeds in the presence of an aperture. For a nano-aperture, this problem was considered in Ref. [33], where rather simple analytical expressions have been found for the case of an arbitrary position of the atom and an arbitrary orientation of its dipole moment. For this problem, it is important that, at any orientation of the atomic dipole moment, radiation at both sides of the plane $z = 0$ can be described by introducing an effective dipole oriented normally to the plane. Moreover, the magnitude of the dipole moment can be different for two dissimilar half-spaces.

Correspondingly, for the total rate of spontaneous decays we obtain

$$\frac{\gamma}{\gamma_0} = \frac{1}{2}\left(\frac{d_{\text{tot}}^{+\,2}}{d_0^2} + \frac{d_{\text{tot}}^{-\,2}}{d_0^2}\right). \tag{15}$$

On the right-hand side of Eqn (15), the first term describes atomic emission into the upper half-space, and the second term into the lower half-space.

The expression for the decay rate becomes very simple in some special cases. For instance, if the atom is placed on the axis of the system (z-axis), emission is possible only for the atom with a dipole moment directed along z. In this case, transition dipole moments describing emission into the upper

and lower half-spaces have the form

$$\frac{d_{\rm tot}^{\pm}}{d_0} = 1 \pm \frac{2}{\pi}\left[\arctan\left(\frac{z}{a}\right) + \frac{az}{a^2+z^2}\right], \qquad (16)$$

where a is the aperture radius.

Dependences of the radiative decay rates on the position of the atom are shown in Fig. 3a. At $z = 0$, one obtains

$$\frac{d_{\rm tot}^{+}}{d_0} = \frac{d_{\rm tot}^{-}}{d_0} = 1\,,$$

i.e., if the atom is at the center of the aperture, its emission is the same as in the case of emission in free space. At $z \to \infty$, we arrive at

$$\frac{d_{\rm tot}^{+}}{d_0} = 2\,, \quad \frac{d_{\rm tot}^{-}}{d_0} = 0\,,$$

and the transition dipole moment corresponding to atomic emission into the upper half-space is doubled. Note that the limit $z \to \infty$ means, of course, only that the following inequalities are valid: $\lambda \gg z \gg a$. If the atom is far enough, so that its separation from the aperture is comparable to the emission wavelength, the nano-aperture does not influence the atomic emission. In this case, the rate of spontaneous decays should be calculated in much the same way as in the presence of a plane without an aperture [8].

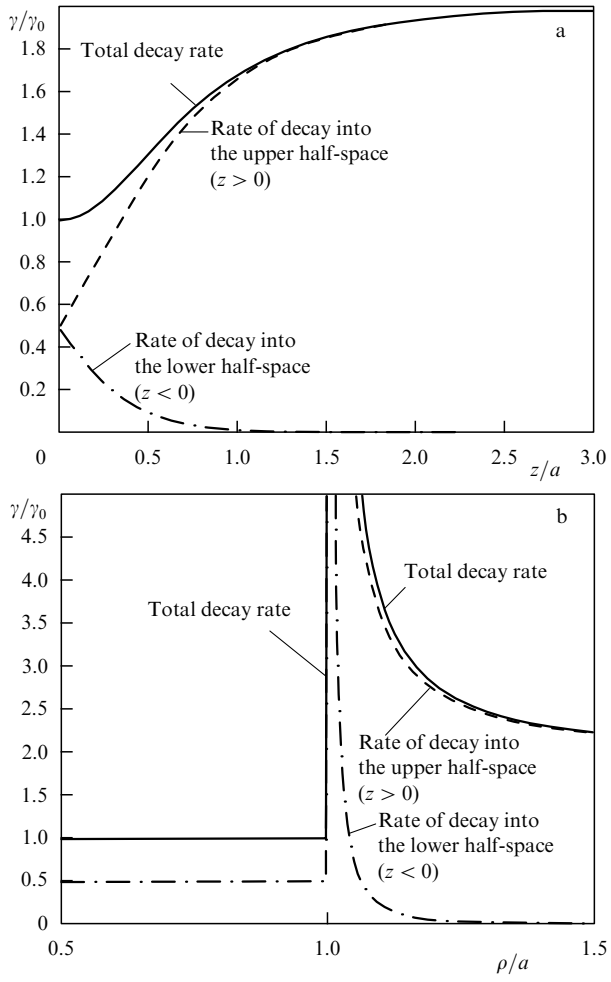

Figure 3. Decay rates as functions of the position for an atom whose dipole moment is normal to the aperture plane: (a) the atom is placed on the axis ($\rho = 0$, $z > 0$), and (b) the atom is placed exactly above the aperture plane ($z = 0^{+}$).

Consider now the decay rate for an atom that is placed in the plane $z = 0^{+}$, its dipole moment being directed along z-axis (Fig. 3b). If the atom resides in the aperture, its radiative decay rate is the same as in the case of the free space at any position of the atom:

$$\frac{d_{\rm tot}^{+}}{d_0} = \frac{d_{\rm tot}^{-}}{d_0} = 1\,.$$

If the atom is placed outside of the aperture ($z \approx 0$, $\rho > a$), then the expressions for the transition dipole moments describing atomic emission to the upper and lower half-spaces take the form

$$\frac{d_{\rm tot}^{\pm}}{d_0} = 1 \pm \frac{2}{\pi}\left(\frac{a}{\sqrt{\rho^2-a^2}} + \arcsin\frac{\sqrt{\rho^2-a^2}}{a\rho}\right), \quad \rho > a\,. \qquad (17)$$

From Eqn (17) it follows that the decay rate in the neighborhood of the aperture edge is increased substantially, with the radiation propagating both in the upper and lower half-spaces.

We will now look at the radiative decay of the atom placed in the plane $z = 0$ and having the ρ-oriented transition dipole moment. (The rate of decays for an atom with φ-oriented dipole moment is equal to zero identically in our approximation.) When $\rho < a$, the formulas for the transition dipole moments describing radiation fields in the upper and lower half-spaces take the form

$$d_{\rm tot}^{\pm} = \mp\frac{2}{\pi}\,\frac{\rho}{\sqrt{a^2-\rho^2}}\,, \quad \rho < a\,. \qquad (18)$$

Outside of the aperture, where $\rho > a$, the total dipole moment is equal to zero due to the boundary conditions for an ideally conducting plane. One can see from Eqn (18) that the decay rate is considerably increased near the edge of the aperture. In this case, there is emission to both upper and lower half-spaces.

6. Spontaneous emission of an atom in the vicinity of an elongated spheroid

Since the problem of atomic emission near a finite-sized spheroid cannot be solved analytically, consider the case where the spheroid is elongated and its sizes are small compared with the emission wavelength. We also assume that the atom is placed close to the spheroid. Then the spontaneous decay rate is determined by the total dipole moment of the system, which can be found by solving the quasi-static problem [34].

When solving the electrostatic problem for an elongated spheroid with semiaxes a, b ($a > b$), it is natural to introduce elongated spheroidal coordinates, the z-axis coinciding with the axis of the system. If the atom possesses the dipole moment aligned with z-axis and is placed at point z on the spheroid axis, then the atomic radiative decay rates are given by the expression

$$\left(\frac{\gamma}{\gamma_0}\right)_{\|} = \left|1 + (\varepsilon - 1) \times \xi_0\left[\xi_0\frac{\rm d}{{\rm d}\xi_0}\,Q_1(\xi_0) - \varepsilon Q_1(\xi_0)\right]^{-1}\frac{\rm d}{{\rm d}\xi}\,Q_1(\xi)\right|^2, \qquad (19)$$

where $\xi_0 = a/\sqrt{a^2 - b^2}$, $\xi = z/\sqrt{a^2 - b^2}$, and $Q_1(x)$ is a Legendre function of the second order.

Note that at some real values of the permittivity, the expression in square brackets in Eqn (19) turns to zero and, hence, there is no solution to the quasi-static problem. As a result, in a manner similar to the case of an insulating sphere, a plasmon resonance arises, which can be described only in the framework of the complete electrodynamic theory. Evidently, this corresponds to a considerable increase in the decay rate [see equation (6)].

We see that from the viewpoint of the influence on the spontaneous emission of an atom, the case of a spheroid is intermediate between the cases of a sphere and a cylinder. This influence enables one to efficiently control the decay rate of an excited atom, including radiative and nonradiative decays. A significant feature of a spheroid is the possibility to 'tune' it, by choosing properly the shape or the ratio of its semiaxes, to the plasmon resonance of any material. This possibility allows us, on the one hand, to control spontaneous radiative decays, and on the other hand, to determine the frequencies of plasmon vibrations for the spheroid material.

A considerable growth in the spontaneous decay rate of an atom in the vicinity of a nanospheroid in the case of plasmon resonance can be used as a basis for operation of an aperture-free scanning microscope with a single molecule as the object of investigation [34]. In such a microscope, the tip can be approximated as an elongated nanospheroid in which it is possible to excite the plasmon resonance at the frequency of the molecular emission. It is supposed that the absorption band of the molecule is far from the plasmon resonance. Preliminary calculations [35] show that such a microscope can measure the position of the molecule with the nanometer resolution, as well as the orientation of the molecular dipole moment. Figure 4 shows the results of simulating the scanning procedure for different orientations of the molecule.

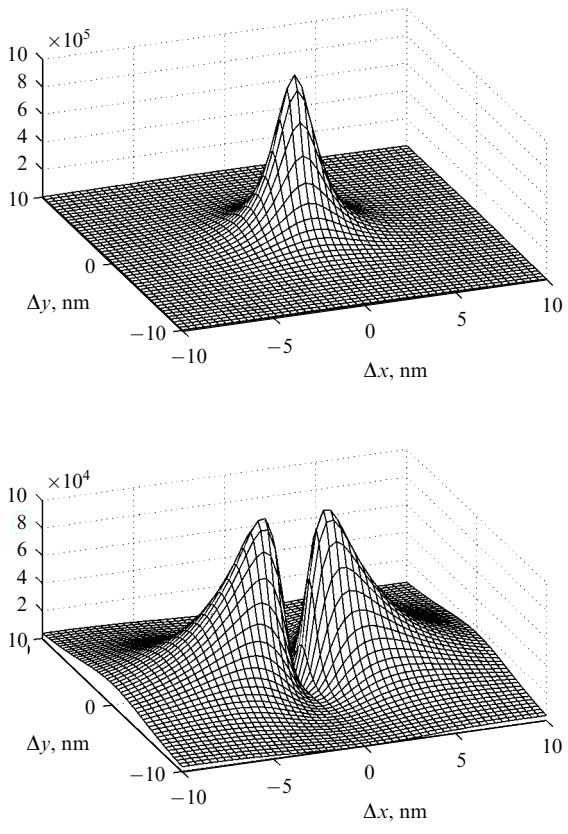

Figure 4. Scanning signals for molecules with different dipole moment orientations. The microscope tip is simulated by a silver nanospheroid [35].

7. Conclusions

The above-developed theory allows one to study other nanobodies, such as a cone [36, 37] or a nanobubble [38]. In all cases, relatively simple analytical expressions can be found for the variation of the spontaneous emission line width and frequency in the vicinity of various nanobodies. The results obtained can be used for developing new types of scanning microscopes with single atoms or molecules as objects of investigation, for the control of atomic motion by means of the near fields of nanobodies, and for the creation of photon sources with given properties. In addition, nanobodies can be utilized for the study of weak quadrupole transitions which become considerably faster in the presence of nanobodies [39].

The author is grateful to the Russian Foundation for Basic Research and to the Federal Program 'Integration' for the financial support of this work.

References

1. Purcell E M *Phys. Rev.* **69** 681 (1946)
2. Bunkin F V, Oraevskiĭ A N *Izv. Vyssh. Ucheb. Zaved. Radiofiz.* **2** (2) 181 (1959)
3. Kleppner D *Phys. Rev. Lett.* **47** 233 (1981)
4. Goy P et al. *Phys. Rev. Lett.* **50** 1903 (1983)
5. Hulet R G, Hilfer E S, Kleppner D *Phys. Rev. Lett.* **55** 2137 (1985)
6. Gabrielse G, Dehmelt H *Phys. Rev. Lett.* **55** 67 (1985)
7. Berman P R (Ed.) *Cavity Quantum Electrodynamics* (Boston: Academic Press, 1994)
8. Haroche S, in *Fundamental Systems in Quantum Optics*: *Les Houches, Session LIII* (Eds J Dalibard, J-M Raimond, J Zinn-Justin) (Amsterdam: North-Holland, 1992) p. 767
9. Jhe W et al. *Phys. Rev. Lett.* **58** 666 (1987)
10. Lin H-B et al. *Phys. Rev. A* **45** 6756 (1992)
11. Pohl D W, Courjon D (Eds) *Near Field Optics* (NATO ASI Series, Ser. E, Vol. 242) (Dordrecht: Kluwer Acad. Publ., 1993)
12. Mohamed M B et al. *Chem. Phys. Lett.* **317** 517 (2000)
13. Lyon W A, Nie S *Anal. Chem.* **69** 3400 (1997)
14. Zander C et al. *Chem. Phys. Lett.* **286** 457 (1998)
15. Denschlag J, Umshaus G, Schmiedmayer J *Phys. Rev. Lett.* **81** 737 (1998)
16. Denschlag J et al. *Appl. Phys. B: Laser Opt.* **69** 291 (1999)
17. Chance R R, Prock A, Sylbey R *Adv. Chem. Phys.* **37** 1 (1978)
18. Klimov V V, Ducloy M, Letokhov V S *Kvantovaya Elektron.* **31** 569 (2001) [*Quantum Electron.* **31** 569 (2001)]
19. Wylie J M, Sipe J E *Phys. Rev. A* **30** 1185 (1984); **32** 2030 (1985)
20. Dung H T, Knöll L, Welsch D-G *Phys. Rev. A* **62** 053804 (2000)
21. Knoll L, Scheel S, Welsch D-G, quant-ph/0006121 (v1)
22. Amos R M, Barnes W L *Phys. Rev. B* **55** 7249 (1997)
23. Drexhage K H, in *Progress in Optics* Vol. 12 (Ed. E Wolf) (Amsterdam: North-Holland, 1974) p. 165
24. Chew H *J. Chem. Phys.* **87** 1355 (1987)
25. Chew H *Phys. Rev. A* **38** 3410 (1988)
26. Klimov V V, Ducloy M, Letokhov V S *J. Mod. Opt.* **43** 549 (1996)
27. Klimov V V, Ducloy M, Letokhov V S *J. Mod. Opt.* **43** 2251 (1996)
28. Klimov V V, Ducloy M, Letokhov V S *Phys. Rev. A* **59** 2996 (1999)
29. Schniepp H, Sandoghdar V *Phys. Rev. Lett.* **89** 257403 (2002)
30. Klimov V V, Ducloy M *Phys. Rev. A* **62** 043818 (2000)
31. Żakowicz W, Janowicz M *Phys. Rev. A* **62** 013820 (2000)
32. Klimov V V, Ducloy M "Spontaneous emission rate of an excited atom placed near a nanofiber", physics/0206048; *Phys. Rev. A* (submitted to publication)
33. Klimov V V *JETP Lett.* **78** 471 (2003)
34. Klimov V V, Ducloy M, Letokhov V S *Eur. Phys. J. D* **20** 133 (2002)

35. Klimov V V, Ducloy M, Letokhov V S *Chem. Phys. Lett.* **358** 192 (2002)
36. Klimov V V *Pis'ma v Zh. Eksp. Teor. Fiz.* **68** 610 (1998) [*JETP Lett.* **68** 641 (1998)]
37. Klimov V V, Perventsev Ya A *Kvantovaya Elektron.* **29** 9 (1999) [*Quantum Electron.* **29** 847 (1999)]
38. Klimov V V, Letokhov V S *Chem. Phys. Lett.* **301** 441 (1999)
39. Klimov V V, Letokhov V S *Phys. Rev. A* **54** 4408 (1996)

PACS numbers: 71.20.Nr, **73.20.–r**

DOI: 10.1070/PU2003v046n09ABEH001645

Electronic properties of narrow gap IV – VI semiconductors

B A Volkov

1. Tight binding approximation to band spectrum model of IV – VI semiconductors

IV – VI semiconductors constitute compounds of elements of group IV (Pb, Sn, and Ge metals) and chalcogenides (Te, Se, S) [1]. They crystallize into an NaCl type structure. The important point, conceptually, is that the electronic spectra and crystal structures of IV – VI compounds are close to those of the bismuth-group semimetals. As in the crystals of group V elements, in IV – VI semiconductors there are, on average, three p-electrons per atom. Two s-electrons form deep narrow bands and do not participate in the actual valence bonds that exist in the crystal. Therefore, the valence and conduction bands should be constructed from p-orbitals (p_x, p_y, p_z) whose cubic symmetry reflects the cubic structure of bonds in IV – VI compounds. If the metal and chalcogene atoms were made chemically identical, their FCC lattice would become a simple cubic lattice with an odd number of (three) electrons per unit cell. According to Luttinger theorem, such a structure must be a metal. It is this praphase which Abrikosov and Fal'kovskiĭ [6] employed to explain the semimetal character of the spectrum of bismuth whose rhombohedral lattice can be considered as a slightly distorted simple cubic one.

A similar approach can conveniently be employed in constructing the electronic spectrum of IV – VI semiconductors by introducing the potential of ionicity into the praphase Hamiltonian — the potential which accounts for the difference between the metal and chalcogene atoms. This potential doubles the period of the simple cubic lattice, with the result that the new (FCC) cell has an even number of electrons ($3 \times 2 = 6$) and its spectrum becomes an insulating one. By order of magnitude, the potential of ionicity is close to the difference between the ionization potentials of the atoms of the metal and chalcogene.

In order to determine the spectrum of the praphase, it is convenient to employ the tight binding approximation by making allowance for the overlap integral taken between the nearest neighboring atoms only. Then, because of the symmetry, this integral will be nonzero only for like atomic p-orbitals, and the spectrum of the praphase will consist of three one-dimensional branches. Each of these will be only half-filled, in which case the Fermi surface of the praphase takes on the appearance of a three-dimensional cross. The symmetry-unrelated degeneracy of the one-dimensional spectrum of the praphase is removed by its interaction with deep s-orbitals and by the intraatomic spin – orbit coupling. This gives rise to a complex Fermi surface consisting of three parts. A nearly-cube-shaped hole surface resides in the center of the praphase's Brillouin zone, whereas at the vertices there are electronic pockets whose total volume is equal to that of the hole surface. In addition, there is also an open Fermi surface. The three surfaces never intersect. As a result of the introduction of ionicity, the whole of the Fermi surface is covered by the gap, giving rise to a real spectrum of semiconducting IV – VI compounds. The above picture of the genesis of the electronic spectrum of IV – VI semiconductors explains, by the way, why it is near the L-points of the Brillouin zone of an FCC lattice that the gap in a IV – VI spectrum is the narrowest. The reason is simply that all Fermi surfaces of the praphase come closest there to one another.

In concluding this section it should be noted that the spectrum of the praphase is not the only point of similarity between the group V semimetals and IV – VI semiconductors. Another is that in some IV – VI semiconductors (GeTe, SnTe) one observes structural transformations from the cubic phase to the rhombohedral (ferroelectric) phase completely similar to the bismuth structure. This occurs when the potential of ionicity is sufficiently small to prevent the deformation of the lattice along the trigonal axis.

2. Dielectric and magnetic properties of IV – VI semiconductors

It is well known that semiconducting IV – VI compounds possess anomalously large values of both the high-frequency (ε_∞) and static (ε_0) dielectric constants. By ε_∞ here is meant the dielectric constant at frequencies higher than all phonon frequencies but much lower than the average ionicity gap. The presence of the narrow gap between the L-points can be ignored because the phase volume corresponding to them is small, whereas that corresponding to transitions across the average ionicity gap is equal to the volume of the Brillouin zone itself. The calculations in Ref. [7] were performed including the local field effects and the exchange correction to vertices.

The essential point is that, as tight binding calculations of IV – VI spectra reveal, the wave functions near the upper and lower edges of the average ionicity gap are of opposite symmetry. States near the upper edge are formed from the atomic functions of the metal and therefore are odd, whereas those near the lower edge are constructed from the atomic functions of the chalcogene, i.e., they are even. The calculations showed that in the cubic phase corrections for the local field are absent, whereas in the rhombohedral phase they are nonzero and proportional to the square of the parameter of rhombohedrality, leading to a drop in the value of ε_∞ with a kink at the phase transition point.

In Ref. [8], the static dielectric constant and effective charge Z^* were calculated. The basic idea was first to determine the polarization of the crystal at fixed displacements of the metal and chalcogene sublattices by taking into account changes in the electron wave functions, and then to use the polarization for finding the static dielectric constant and the effective charge Z^*. It turned out that the effective charge grows as the degree of ionicity decreases. This

[1] The results of my work with the colleagues, both theoreticians and experimenters, can be found in reviews [1 – 5] where they are discussed in detail, and in a number of separate original papers on the dielectric and magnetic properties of IV – VI semiconductors [6 – 10].